Identification and Functional Assessment of Age-Dependent Truncations to Cx46 and Cx50 in the Human Lens

Nefeli Slavi,[1] Zhen Wang,[2] Lucas Harvey,[1] Kevin L. Schey,[2] and Miduturu Srinivas[1]

[1]Department of Biological and Vision Sciences and the Graduate Center for Vision Research, SUNY College of Optometry, New York, New York, United States
[2]Department of Biochemistry and Mass Spectrometry Research Center Vanderbilt University School of Medicine, Nashville, Tennessee, United States

Correspondence: Miduturu Srinivas, Department of Biological and Vision Sciences, SUNY State College of Optometry, 33 West 42nd Street, New York, NY 10036, USA; msrinivas@sunyopt.edu.

Submitted: April 5, 2016
Accepted: August 21, 2016

Citation: Slavi N, Wang Z, Harvey L, Schey KL, Srinivas M. Identification and functional assessment of age-dependent truncations to Cx46 and Cx50 in the human lens. *Invest Ophthalmol Vis Sci*. 2016;57:5714–5722. DOI:10.1167/iovs.16-19698

Purpose. Many proteins in the lens undergo extensive posttranslational modifications (PTMs) with age, leading to alterations in their function. The extent to which lens gap junction proteins, Cx46 and Cx50, accumulate PTMs with aging is not known. In this study, we identified truncations in Cx46 and Cx50 in the human lens using mass spectrometry. We also examined the effect of truncations on channel function using electrophysiological measurements.

Methods. Human lenses were dissected into cortex, outer nucleus, and nucleus regions, and fiber cell membranes were subjected to trypsin digestion. Tryptic peptides were analyzed by liquid chromatography (LC)–electrospray tandem mass spectrometry (ESI/MS/MS). Effects of truncations on channel conductance, permeability, and gating were assessed in transfected cells.

Results. Cleavage sites were identified in the C-terminus, the cytoplasmic loop, and the N-terminus of Cx46 and Cx50. Levels of C-terminal truncations, which were found at residues 238 to 251 in Cx46 and at residues 238 to 253 and 274 to 284 in Cx50, were similar in different lens regions. In contrast, levels of truncations in cytoplasmic loop and N-terminal domains of Cx46 and Cx50 increased dramatically from outer cortex to nucleus. Most of the C-terminally truncated proteins were functional, whereas truncations in the cytoplasmic loop did not result in the formation of functional channels.

Conclusions. Accumulation of cytoplasmic loop and N-terminal truncations in the core might lead to decreases in coupling with age. This reduction is expected to lead to an increase in intracellular calcium and a decrease in levels of glutathione in the nucleus. These changes may ultimately lead to age-related nuclear cataracts.

Keywords: posttranslational modifications, connexins, gap junctions, mass spectrometry

Intercellular communication mediated by gap junction (GJ) channels is required for postnatal lens growth and for the maintenance of lens transparency. These cell–cell channels mediate direct signaling between cells and are formed by the docking of two hemichannels, one from each of two contacting cells. Each hemichannel is a hexamer of connexin subunits, with a topology that consists of four transmembrane (TM) domains (TM1–TM4) and two extracellular loops (EL1 and EL2) with the amino and carboxyl termini located intracellularly.[1] The lens expresses three connexin family members (Cx43, Cx46, and Cx50) in distinct spatial and overlapping patterns. Cx43 is exclusively expressed in the epithelium,[2,3] whereas Cx46 is present only in fiber cells, where its expression coincides with fiber cell differentiation.[4] Cx50 is present in both epithelial cells and fibers.[5–8]

The importance of GJ coupling for lens homeostasis is highlighted by the association of mutations in Cx46 and Cx50 genes to the development of cataracts,[9,10] and from studies in mice lacking connexin proteins.[6,11,12] Gap junction channels are important components of the lens microcirculation system, which is critical for the movement of water and solutes through the lens and, thus, for lens homeostasis.[13,14] Loss of GJ coupling in central fibers, as observed in lenses from Cx46 knockout mice,[15] disrupts the microcirculation and leads to increases in intracellular calcium in central fiber cells and a central cataract.[11,16–18] Lens GJ channels are also permeable to antioxidant molecules, such as glutathione.[19] Therefore, they can contribute to the delivery of the antioxidant from outer fiber cells,[19,20] where a high concentration is established by synthesis or uptake,[21–24] to central fiber cells, which have minimal capacity for glutathione synthesis.

Like other proteins in the lens, Cx46 and Cx50 undergo age-dependent posttranslation modifications (PTMs). This is due to the unique pattern of lens growth and development.[25] Differentiation of epithelial cells into fiber cells occurs throughout life and produces concentric layers of fibers, with the oldest fiber cells in the lens center and the youngest cells in the lens periphery. Fiber cells lose their nuclei and other organelles during the course of differentiation.[26] Turnover of proteins is virtually nonexistent following terminal differentia-

Investigative Ophthalmology & Visual Science

tion,[27] and, thus, many proteins in mature fiber cells accumulate age-dependent truncations, deamination, oxidation, racemization, and glycation, leading to changes in protein function.[28–32] Biochemical studies indicate that the C-termini of Cx46 and Cx50 are cleaved during the course of differentiation, and in the case of Cx50, these truncations were attributed to the enzymatic action of calpain or of caspases.[33–37] Several truncation and phosphorylation sites in bovine Cx46 and Cx50 were also identified by mass spectrometry.[38–40] However, the spatial distribution of the truncated forms of Cx46 and Cx50 has been examined in only one study, which showed that, in bovine lenses, some cleavage sites were observed at a higher prevalence in the nucleus than in the cortex.[38–40] No data are available on the specific sites of truncation in human lenses, their distributions within the lens, or their relative abundances.

The purpose of this study was to identify sites of truncation and to determine whether truncations to Cx46 and Cx50 increase in human lenses with fiber cell age. Human lenses were concentrically dissected into regions of varying fiber cell age and the sites of backbone cleavage were determined by mass spectrometry. Use of more sensitive technologies allowed us to map the relative incidence of each modification in different regions of the lens. An additional purpose of our study was to characterize the effects of truncations on channel properties. There are a large number of studies detailing the functional properties of truncated connexin channels; however, these functional studies thus far have focused on the consequences of cleavage of the Cx50 C-terminal domain by calpains or caspases.[41–46] The functional consequences of endogenous Cx46 truncations have not been examined in previous studies. Here, we determined whether Cx46 and Cx50 truncations identified in the human lens affect functional properties of the resulting GJ channels using electrophysiological techniques.

Materials and Methods

Membrane Preparation and Trypsin Digestion

Human lenses were obtained from NDRI (Philadelphia, PA, USA). All lenses were isolated from the donor no later than 8 hours post mortem, shipped frozen and stored at –80°C before dissection. Fifty-five and 62-year-old human lenses were decapsulated and dissected into cortex (outer 0.5 mm of tissue), outer nucleus (approximately 1 mm wide ring inside of cortex containing adult nucleus and juvenile nucleus), and nucleus regions (remaining core tissue containing fetal nucleus and embryonic nucleus)[47] by pulling away each layer of tissue with tweezers. A second set of lenses was dissected using Acupunch surgical trephines (Acuderm, Inc., Ft. Lauderdale, FL, USA), as described in the Supplementary Information. All dissected tissue was processed identically. Each sample was homogenized in homogenizing buffer (25 mM Tris, 150 mM NaCl, 5 mM EDTA, 1 mM dithiothreitol (DTT), and 1 mM phenylmethylsulfonyl fluoride (PMSF), pH 7.5). After homogenization, the sample was centrifuged at 100,000*g* for 30 minutes and the supernatant was discarded. The pellets were washed twice with the above homogenizing buffer followed by three washes with homogenizing buffer containing 8 M urea to obtain the urea-insoluble fraction (UIF). The UIF was further washed with 0.1 M NaOH followed by one water wash. Centrifugation at 100,000*g* was performed to separate the supernatant and pellets for each wash. The final pellets were suspended in 100 μL water; 5 μL was saved for protein assay. For protein assay, a 5 μL aliquot of sample was mixed with 5 μL 5% SDS and protein concentration was measured by bicinchoninic acid assay (Thermo Scientific, Rockford, IL, USA). An aliquot of 1 μL 1 M DTT was added to the remaining sample and incubated at 56°C for 1 hour to reduce disulfide bonds. An aliquot of 10 μL of 500 mM iodoacetic acid (IAA) was then added and the sample was incubated at room temperature for 45 minutes in the dark to alkylate free cysteines. The sample was then centrifuged at 100,000*g* for 30 minutes and the pellets were saved. The pellets were suspended in 50 mM Tris (pH 8.0) containing 10% acetonitrile and digested by trypsin for 18 hours at 37°C. After digestion, the sample was dried in a SpeedVac (model SPD131DDA, ThermoScientific, Milford, MA, USA). Peptides were reconstituted in 0.1% formic acid (0.5 μg/μL) for mass spectrometry analysis.

Liquid Chromatography-Electrospray Ionization-Tandem MS (LC-ESI/MS/MS)

Tryptic peptides corresponding to 1 μg total protein were separated on a one-dimensional fused silica capillary column (200 mm × 100 μm) packed with Phenomenex (Torrance, CA, USA) Jupiter resin (3 μm mean particle size, 300 Å pore size) coupled with an Eksigent nanoHPLC system (Eksigent Technologies, Dublin, CA, USA). A 145-minute gradient elution was performed, consisting of the following gradient: 0 to 12 minutes, 2% B; 12 to 127 minutes, 2% to 40% B; 127 to 132 minutes, 40% to 95% B; 132 to 133 minutes, 95% to 2% B; 133 to 145 minutes, 2% B. The eluate was directly infused into a Q Exactive instrument (ThermoScientific, San Jose, CA, USA) equipped with a nanoelectrospray source. The instrument method consisted of MS1 acquisition ($R = 70{,}000$) followed by up to 18 MS/MS scans ($R = 17{,}500$) of the most abundant ions detected in the preceding MS1 scan. The MS2 automatic gain control target value was set to 5e4 ions, with a maximum ion time of 120 ms and an 8% underfill ratio. The higher energy collisional dissociation collision energy was set to 26, dynamic exclusion was set to 20 seconds, and peptide match and isotope exclusion were enabled.

Data Analysis

To obtain the relative abundance of truncation at each site, the selected ion chromatograms for truncated peptides and corresponding untruncated tryptic peptides were generated using 5 ppm mass accuracy. Peak areas were calculated using the Genesis peak algorithm within the Xcalibur software 2.2 SP 1.48 (ThermoFisher, San Jose, CA, USA). The relative abundance of truncation was expressed as the ratio of peak area of truncated peptide relative to the peak area of the corresponding untruncated tryptic peptide.

Transient Transfection

Human Cx50 and human Cx46 were cloned into the pCS2^{+} and piRES2-GFP expression vectors, respectively. Truncations were generated by inserting a stop codon after the indicated amino acid residues in the connexin cDNA. The truncations that were tested for functionality included H253tr and G110tr in Cx50 and D251tr and N129tr in Cx46. All truncations were constructed using the QuikChange mutagenesis kit (Stratagene, La Jolla, CA, USA) in accordance with manufacturer's protocol using the full-length connexin expression constructs as templates. All constructs were verified by sequencing. HeLa cells were transiently cotransfected with 400 ng full-length and truncated cDNA in combination along with mCherry plasmid (Clontech Laboratories, Inc., Mountain View, CA, USA) using Lipofectamine 2000 reagent (Invitrogen, Carlsbad, CA, USA). Cells were plated at low density onto glass coverslips; DNA

Investigative Ophthalmology & Visual Science

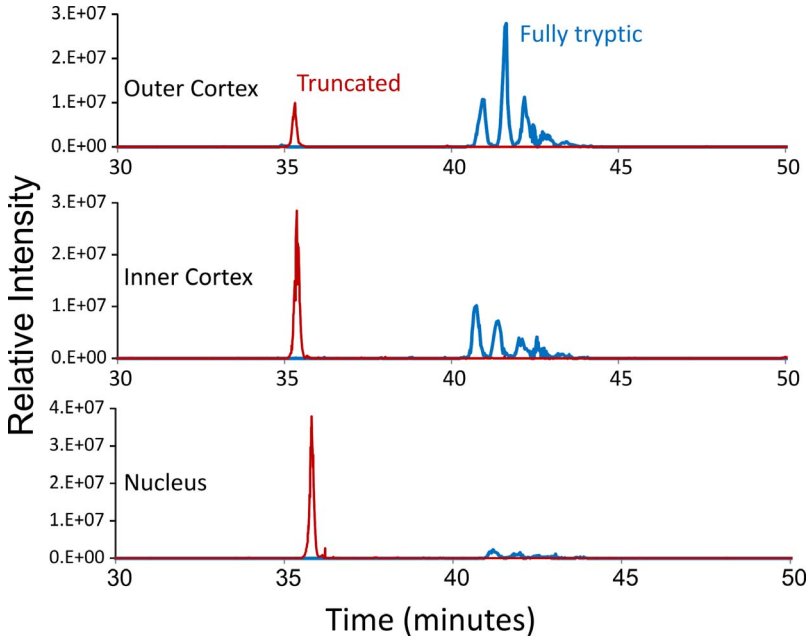

Figure 1. Separation of tryptic peptides of Cx50 from different regions of a 55-year-old lens. The selected ion chromatograms for tryptic peptide 110 to 130 (*blue*) and nontryptic peptide 110 to 119 (*red*) in samples from different regions of the lens. Multiple peaks for 110 to 130 were due to isomerization of aspartic acids in the peptides, which are not in the truncated peptides. The relative level of peptide 110 to 119 (truncated) with respect to 110 to 130 (full length) dramatically increases from cortex to nucleus. In the lens nucleus, Cx50 was significantly truncated in this region and the full-length peptide was barely detected.

concentrations were measured using Nanodrop 2000 (ThermoScientific).

Electrophysiology

Junctional conductance was measured between HeLa cell pairs by using the dual whole-cell voltage clamp technique with Axopatch 1D patch-clamp amplifiers (Axon Instruments, Foster City, CA, USA). The solution bathing the cells contained (in mM) 140 NaCl, 5 KCl, 2 CsCl, 2 $CaCl_2$, 1 $MgCl_2$, 5 HEPES, 5 dextrose, 2 pyruvate, and 1 $BaCl_2$, pH 7.4. Patch electrodes had resistances of 3 to 5 MΩ when filled with internal solution containing (in mM) 130 CsCl, 10 EGTA, 0.5 $CaCl_2$, and 10 HEPES, pH 7.2. Macroscopic and single-channel recordings were filtered at 0.2 to 0.5 kHz and sampled at 1 to 2 kHz. Each cell of a pair was initially held at a common holding potential of 0 mV. To evaluate junctional coupling, 200-ms hyperpolarizing pulses from the holding potential of 0 mV to −20 mV were applied to one cell to establish a transjunctional voltage gradient (V_j), and junctional current was measured in the second cell (held at 0 mV). Single-channel currents were investigated in weakly coupled cell pairs (one or two channels) by applying −20-mV pulses to one cell of a pair. Data were acquired by using pCLAMP9.2 software (Molecular Devices, Sunnyvale, CA, USA); analysis was performed with pCLAMP9.2 and ORIGIN 6.0 software (Microcal Software, Northampton, MA, USA).

Results

LC–MS/MS Analysis of Cx46 and Cx50 Truncation in Human Lens Regions

Truncation sites of Cx46 and Cx50 were identified by automated searching for nontryptic peptides in the LC-MS/MS datasets. Both Cx46 and Cx50 were found to be truncated at Gly 2 as previously reported in bovine lens.[38–40] Truncation at Gly 2 has been confirmed by an N-terminal dimethylation experiment before trypsin digestion to rule out nonspecific trypsin cleavage (data not shown). No further experiments were done to rule out nonspecific trypsin cleavage for other truncation sites identified; however, truncation sites identified either showed a clear difference among samples from different regions of the lens or were clustered in specific regions of the protein, suggesting protein truncation. In all four human lenses analyzed, cleavage of Cx46 was repeatedly found in the cytoplasmic loop (Q127, D128, N129) and the cytoplasmic tail adjacent to the last transmembrane domain (D241, A242, A250, D251) (see Figs. 2A, 3A for a connexin topology diagram showing the location of sites). Truncation of Cx50 was also repeatedly detected in the cytoplasmic loop (Q117, G119, N121, G122, G123, D125, Q126, and G127) and the cytoplasmic tail (E246, S251, H253, V275, S276, H277, E283, and V284) (see Figs. 2A, 3A). Figure 1 shows an example of extracted ion chromatograms of truncated and full-length Cx50 peptides corresponding to the cytoplasmic loop highlighting the changes in truncated Cx50 with age.

C-Terminal Truncations and Their Prevalence in the Different Regions of the Lens

The level of truncation in the C-terminus of Cx46 and Cx50 in the cortex, outer nucleus, and nucleus from a 55-year-old human lens was quantified and the results are shown in Figure 2. Multiple sites of truncation in the C-terminus, adjacent to the last transmembrane domain, were detected for both Cx46 and Cx50. Tandem mass spectra of the abundant truncated Cx46 and Cx50 peptides are shown in Supplementary Materials (Supplementary Figs. S3–S5). In Cx46, the main backbone cleavage site in this region is at aspartic acid 251. Truncation at D251 was observed in membrane fractions obtained from the cortex, indicating that the posttranslational modification of Cx46 occurs in younger differentiating fibers in the lens (Fig. 2B), consistent with previous immunocytochemical studies.[33]

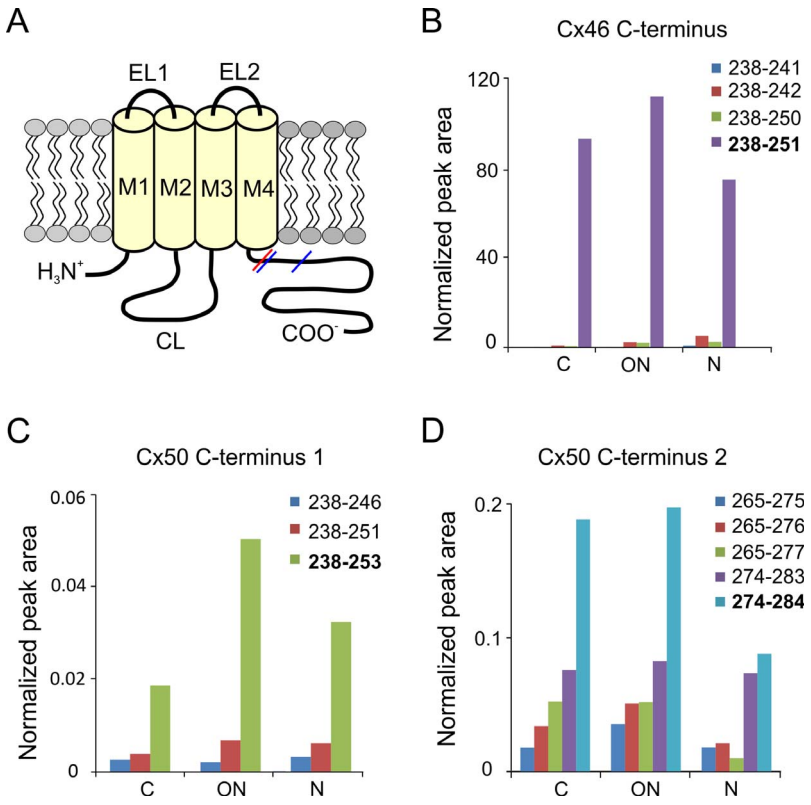

Figure 2. Cleavage sites in the C-termini of Cx46 and Cx50 in a 55-year-old human lens. (**A**) Schematic drawing of the connexin membrane topology indicating the sites of truncation in Cx46 (*red*) and Cx50 (*blue*) in the C-terminus. *CL*, cytoplasmic loop; *EL1*, *EL2*, extracellular domains; *TM1–TM4*, transmembrane domains. Truncation of the C-termini was found in samples obtained from the cortex (C), outer nucleus (ON), and the nucleus (N). Cleavage sites adjacent to the fourth transmembrane domain were found in Cx46 (**B**) and Cx50 (**C**). Peak areas of nontryptic Cx46 peptides (**B**) were normalized to peak area of Cx46 peptide 10 to 23 because the full-length tryptic peptide was too long to show good signal in MS. Peak areas for Cx50 peptides (**C**) were normalized to peak area of Cx50 peptide 238 to 250. Truncation at H253 and S251 results in very short, undetectable tryptic peptides due to a lysine at position 250; therefore, only the miscleaved tryptic peptides (238–251 and 238–253) were detected as truncation products. Because the normalized peak areas shown in (**C**) were calculated by comparing the miscleaved truncated peptides to the fully tryptic peptide (251–262), differences in ionization efficiencies could occur and, therefore, the low normalized peak areas do not necessarily indicate a low prevalence of truncation at these sites. The Cx50 C-terminus was also cleaved at multiple locations between residues 274 and 284 (**D**), and the signal was normalized to peak area of Cx50 265 to 273. The major truncated products are indicated in *bold*. The relative abundance of Cx46 and Cx50 truncations did not change in the different regions of the lens.

The levels of the D251 truncation remained relatively constant in the cortex, outer nucleus, and nucleus. In Cx50, truncations in the carboxyl tail were found at two different regions of the protein. Backbone cleavage at H253 and S251, adjacent to TM4, was observed (Fig. 2C). In addition, a number of truncation sites were located in the region between residues 270 and 290 (Fig. 2D), a highly conserved region of Cx50 that is also the site of enzymatic action of calpain.[34,35] Previous studies in ovine and bovine Cx50 have identified residue 290 as a major cleavage site.[34,35,38,39] In the human lens, the predominant truncation sites were identified at V284 and E283 (the conserved site for E290 in bovine and sheep Cx50). As observed with Cx46, truncations at the two sites in the carboxyl tail of Cx50 occurs at an early age and showed no significant age-dependent alterations in their levels (Figs. 2C, 2D). Similar results were obtained from 19-, 22-, and 62-year old lenses (see Supplementary Figs. S1, S2 for data obtained from relatively younger lenses).

Truncations in the Cytoplasmic Loop and N-terminus Show an Increase With Fiber Cell Age

Several cleavage sites in the cytoplasmic loop region adjacent to TM2 were found in Cx46 and Cx50 (Fig. 3). These cleavage sites were located in the region between residues 118 and 129 in Cx46 (Fig. 3B) and between residues 110 to 127 in Cx50 (Fig. 3C). In both Cx46 and Cx50, levels of the truncations in the cytoplasmic loop increased dramatically with fiber cell age. The signal for N129, the most abundant truncation in Cx46, was weak in the outer cortex, but increased significantly in the inner cortex and even further in the nucleus (Fig. 3B). Similarly, the major site of truncation at G119 in the cytoplasmic loop of Cx50 was found to be much higher in the inner cortex and the nucleus than in the outer cortex (Fig. 3C). In the 55-year-old lens, the levels of N129 and G119 truncations were 20- to 200-fold higher in the samples from the lens core compared with those found from the outer cortex. Tandem mass spectra of the Cx50 and Cx46 peptides truncated in the cytoplasmic loop domains are shown in the Supplementary Materials. Similar results were obtained from a 62-year-old lens (data not shown). In younger lenses, the levels of these truncations also showed a large increase in the nucleus compared with the cortex (Supplementary Figs. S1, S2). However, the levels of the cytoplasmic loop truncations are substantially lower than in the older lenses, suggesting that accumulation of these cleavage events increases progressively with the age of the lens.

In addition, mass spectrometric studies revealed a cleavage site at the N-terminal glycine at residue 2 in Cx46 (Fig. 3D). The levels of this truncation showed a strong increase in older

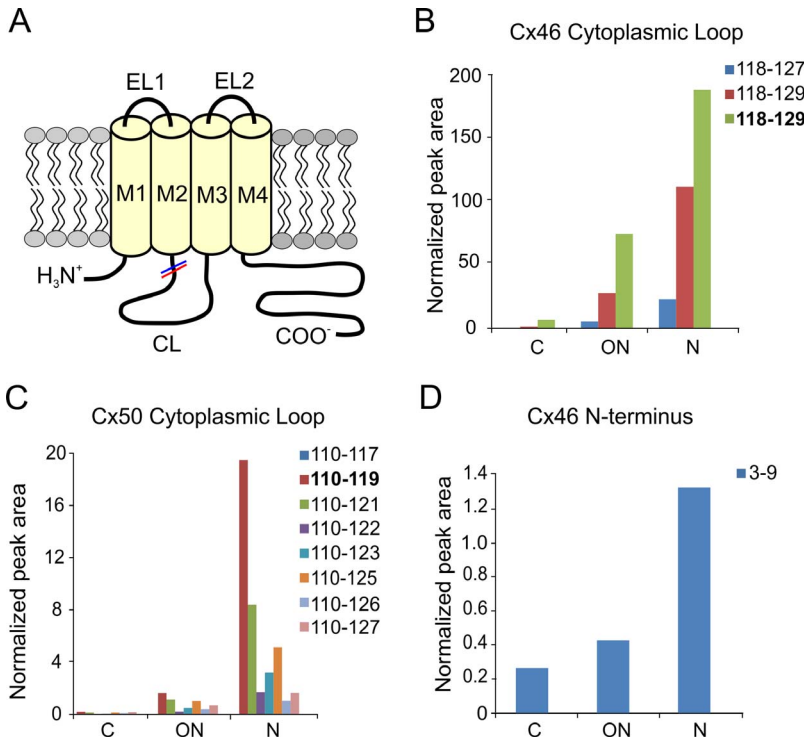

Figure 3. Cleavage sites in the cytoplasmic loop and the N-terminal domains of Cx46 and Cx50. (**A**) Schematic drawing of the connexin membrane topology indicating the sites of truncation in Cx46 (*red*) and Cx50 (*blue*) in the cytoplasmic loop and N-terminus. Truncations in the cytoplasmic loop were found in several sites between residues 118 and 129 in Cx46 (**B**) and the signal was normalized to peak area of Cx46 118 to 133. Truncations in the cytoplasmic loop of Cx50 were found in region 110 to 125 (**C**) and the signal was normalized to peak area of Cx50 110 to 130. In addition, a cleavage site at the N-terminal glycine was detected in the lens (**D**) and the signal was normalized to peak area of Cx46 peptide 2 to 9. The major truncated products are indicated in bold. Levels of cytoplasmic loop and N-terminal truncations in Cx50 and Cx46 were low in abundance in samples obtained from the cortex (C) but increased significantly in the ON and N.

fiber cells compared with newly formed cells (see Supplementary Materials for tandem mass spectra).

Effect of Truncations on Junctional Conductance

The electrophysiological properties of channels formed by C-terminal truncations were examined in transiently transfected HeLa cells. Only those truncations that were detected at a relatively high prevalence in the human lens were characterized. These included C-terminal truncations at D251 in Cx46 and at H253 and V284 in Cx50. The effects of cytoplasmic loop truncations at N129 in Cx46 and at G119 in Cx50 were also studied. Junctional conductances in cells expressing truncated subunits and full-length Cx46 and Cx50 are shown in Figure 4. Junctional conductance was measured by applying brief voltage pulses to −20 mV from a holding potential of 0 mV to one cell of a pair. Full-length Cx46 formed functional intercellular channels with a mean conductance of 6.2 nS (Fig. 4A). In comparison, cells transfected with Cx46_D251 exhibited a mean conductance value of 4.5 nS ($n = 21$), indicating a modest, but not statistically significant reduction compared with full-length Cx46 ($P > 0.05$). The effect of the H253 and V284 truncations in Cx50 on junctional conductance is illustrated in Figure 4B. Expression of H253 truncation resulted in cells that were robustly coupled with values similar to those expressing full-length Cx50 (G_j ~16.5 ± 5.3 nS; $n =$ 35 for H253 truncation and ~24.2 ± 5.6 nS; $n = 39$ for Cx50 [$P > 0.05$]). In contrast, cell pairs expressing the shorter V284 truncation were not coupled ($n = 18$), confirming previous results in N2A cells. These results indicate that domains between residues 253 and 284 in human Cx50 modulate trafficking and/or channel functionality, as reported previously for rodent Cx50.[48] Additional studies to identify the specific amino acids involved in this effect were not pursued because of the absence of anti-Cx50 antibodies that target other domains of the protein.

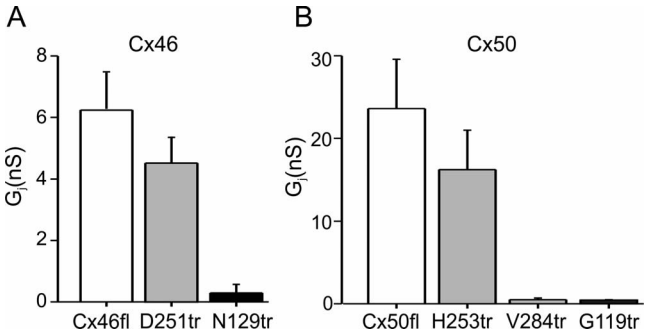

Figure 4. Effect of Cx46 and Cx50 truncations on coupling levels in HeLa cells. *Bar graphs* show the G_j values in HeLa cells transfected with cDNA corresponding to full-length Cx46 and Cx50 (*light bars*) as well as C-terminal truncations (*gray bars*) and cytoplasmic loop truncations (*dark bars*) in Cx46 and Cx50. Junctional conductance values in cells expressing the C-terminal truncations of Cx46 (**A**) and Cx50 (**B**) at residues 251 and 253, respectively, were comparable to those expressing their full-length counterparts. In contrast, the V284 truncation in Cx50 did not form functional intercellular channels. Junctional conductance (G_j) values in cells transfected with cDNA transfected with cytoplasmic loop truncations had very low levels of coupling, and not higher than those found in untransfected parental cells (data not shown). Each *bar* represents the mean ± SEM from multiple cells pairs, as described in the text.

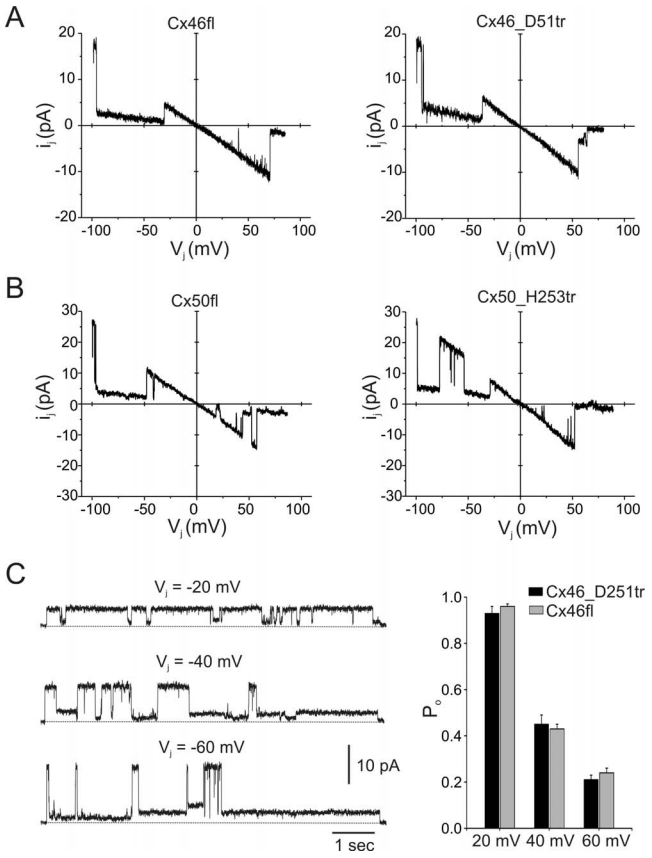

Figure 5. C-terminal truncations do not affect single-channel conductance or open probability. (**A**, **B**) Single-channel current-voltage relationships from cell pairs expressing full-length (fl) and truncated Cx46 (**A**) and Cx50 channels (**B**). I-V relations were obtained in response to 8-second voltage ramps from −100 to +80 mV applied to one cell of a pair. Single channels from cells expressing D251 truncation in Cx46 had a similar slope conductance of approximately 195 pS in comparison with full-length Cx46, which formed channels with a unitary conductance of 190 pS. Slope conductances of cells expressing full-length Cx50 and H253_Cx50 truncation are 272 pS and 279 pS, respectively. (**C**) Recordings of single D251 truncated channel currents at transjunctional voltages of −20, −40, and −60 mV are shown (*left*). Channels of Cx46_D251tr were primarily open at −20 mV but transitioned to lower conductance states at −40 mV and −60 mV. The closed state in current traces is indicated by a *dotted line*. The voltage-dependent changes in channel P_o of D251tr and full-length Cx46 channels were similar in magnitude (*right*). Each *bar* represents the mean ± SEM from three to four cell pairs.

As shown in Figure 4, truncations in the cytoplasmic loop at N129 in Cx46 ($n = 21$) and at G119 in Cx50 ($n = 24$) impaired intercellular coupling in transfected cells. This result is not particularly surprising because subunits missing nearly two-thirds of the protein are unlikely to traffic to the plasma membrane and if trafficking does occur, full oligomerization to form functional channels is unlikely. This is a limitation of studies in transfected cells; it is unlikely that altered trafficking plays a role in the lens because cleavage is a postmembrane insertion event in the lens.

Effect of the Backbone Cleavage of Cx46 and Cx50 on Single-Channel Properties

We determined whether Cx46 and Cx50 truncations affected single-channel conductance, ionic permeability, and channel open probability (P_o). To examine whether the carboxyl tail of Cx46 and Cx50 affected these parameters, current traces were recorded from poorly coupled cell pairs expressing full-length or truncated connexin subunits. Representative single-channel current traces in cells expressing full-length and truncated Cx46 in response to voltage ramps from −100 mV and +100 mV are illustrated in Figure 5A. The unitary conductances of channels formed by full-length Cx46 and D251 truncation, measured as the slope conductance at 0 mV, were 190 pS and 195 pS, respectively. Analysis of unitary current amplitudes from multiple cell pairs yielded a mean single-channel conductance of 189 ± 5 pS ($n = 5$) for full-length Cx46 channels and 192 ± 4 pS ($n = 8$) for truncated D251 channels, indicating no significant differences ($P > 0.05$). Similarly, truncation at H253 in Cx50 did not affect the single-channel conductance of Cx50 GJ channels (Fig. 5B). Slope conductances of cells expressing full-length Cx50 and H253_Cx50 truncation are 272 pS and 279 pS, respectively. We also determined whether C-terminal truncation altered permeability. Measurements of reversal potentials using NaCl gradients indicated that the removal of the C-termini of Cx46 and Cx50 did not affect the relative permeabilities of channels to Na^+ and Cl^- (data not shown). These results are consistent with previous studies that localize the pore-lining elements in the N-terminus, TM1, and EL1 domains of the connexin proteins.[49,50]

The effect of C-terminal truncations on voltage gating was examined by measuring P_o of junctional currents in response to a series of voltage pulses to one cell of a pair. Figure 5C shows recordings of single homotypic GJ channels in cells expressing D251 truncation at V_j of −20 mV, −40 mV, and −60 mV. Truncated Cx46 channels are predominantly open at low transjunctional voltage gradients, but exhibited closures to subconductance states or fully closed states with increasing voltage gradients (Fig. 5C). In this particular example, the channel P_o declined from approximately 0.87 at −20 mV to 0.4 and 0.21 at −40 and −60 mV, respectively. The mean P_o values of D251 truncated channels at the three different voltages were comparable to those obtained from cells expressing full-length Cx46 (Fig. 5C, right). These results indicate that truncation of the carboxyl tail at residue 251 did not affect the voltage gating of Cx46. Similarly, truncation at H253 in Cx50 did not affect the P_o of Cx50 GJ channels (data not shown).

Gating of Truncated Channels by Intracellular Acidification

The intracellular pH in inner lens fibers is more acidic than that in the cortex. Impedance studies in intact lenses have shown that GJ conductance between the fiber cells in the core is poorly sensitive to intracellular acidification by 100% CO_2. In addition, studies in lenses from connexin knockout mice or in the presence of Cx50-selective inhibitors indicated that gating by low pH requires Cx50.[51–53] Cx46 channels in the lens lacked intrinsic pH sensitivity, an effect that was attributed to posttranslational processing of Cx46.[51–53] Therefore, we examined whether C-terminal truncation of Cx46 renders channels incapable of responding to low pH. Figure 6 shows the effect of perfusion of 100% CO_2-saturated external solution to cell pairs expressing truncated connexin subunits on junctional conductance. Cell pairs expressing full-length and truncated channels exhibited a rapid decline in GJ conductance on perfusion with 100% CO_2. The effect of intracellular pH was completely reversible on exposure of cell pairs to CO_2-free solutions. Similar results were obtained in other cell pairs, with CO_2 producing a reduction of 98% to 100% on average in the GJ conductance in cells expressing full-length ($n = 5$) and truncated Cx46 subunits ($n = 6$). These results indicate that C-

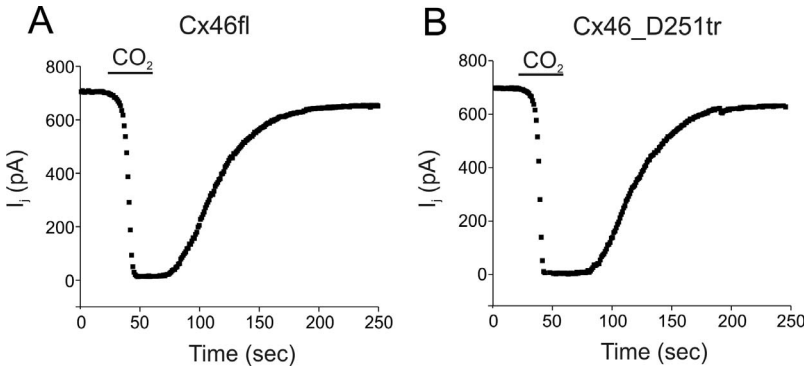

Figure 6. pH gating of full-length and truncated Cx46 channels. Effect of 100% CO_2 on the G_j in cell pairs expressing full-length Cx46 (**A**) or Cx46_D251tr (**B**) subunits. Channels of Cx46_D251tr rapidly closed during cytoplasmic acidification with similar-onset kinetics as full-length Cx46, indicating that C-terminal truncation did not eliminate pH gating. Junctional conductance recovered to control values on washout of CO_2. Similar results were obtained in four to five other cell pairs.

terminal truncation of human Cx46 or Cx50 does not affect the pH gating properties of GJ channels in HeLa cells.

Discussion

In this study, we identified the PTMs to human lens Cx46 and Cx50 that accrue with age. Using LC-MS/MS, sites of backbone truncation were mapped for the first time in human Cx46 and Cx50 as a function of fiber cell age. Analysis of peptides generated by trypsin cleavage in two different human lenses revealed that truncations of Cx46 and Cx50 occur due to cleavage at specific sites within the C-terminal, cytoplasmic loop, and the N-terminal domains. Cleavage in the C-terminal region in both Cx46 and Cx50 occurred in differentiating fiber cells, consistent with previous reports in the rodent lens.[33] Both Cx46 and Cx50 underwent additional truncations in the cytoplasmic loop and the N-terminus. The relative abundance of these truncations showed a marked change with fiber cell age, with the highest level of truncation products occurring in the oldest fibers of the nucleus and the lowest levels occurring in the younger differentiating fiber cells in the outer cortex. The pattern and spatial distribution of Cx46 and Cx50 truncation products were similar in the lenses studied, implying that these modifications are normal consequences of aging and not due to random events.

Our results suggest that intercellular communication in the lens core is mediated by channels that are composed of a mixture of connexin subunits cleaved at the C-terminus and at the other cytoplasmic domains. It is likely that the ratio of the different truncations in individual connexin hemichannels is dependent on the age of the lens. At early developmental time points, coupling might be provided by channels that are predominantly composed of connexin subunits cleaved at the C-terminus. With increasing age, Cx46 and Cx50 undergo gradual accrual of truncations in the cytoplasmic loop and N-terminal domains. Our experiments, which were conducted in lenses obtained from relatively young and older lenses, provide some information about the aging of Cx46 and Cx50 over time. In younger lenses, the levels of the age-related truncations were lower than those found in older lenses. Additional studies in even younger lenses will help determine whether levels of cytoplasmic loop and N-terminal truncations show a gradual age-dependent increase in the lens core.

Previous studies in the rodent lens indicated that cleavage of the C-termini of Cx46 and Cx50 coincides with the loss of organelles and nuclei, and correlates with a 50% reduction in GJ channel conductance in the lens at the differentiating-to-mature fiber transition.[37,52] Cleavage of the Cx50 C-terminus appears to cause a reduction in the contribution of this connexin isoform to lenticular coupling, leaving truncated Cx46 channels to provide GJ-mediated communication in fully differentiated fiber cells.[15,51–54] Previous studies in expression systems indicate that calpain cleavage of Cx50 at the two closely spaced sites in the C-terminus results in either a loss of function or a large reduction in GJ conductance.[41–45] The large reduction in coupling levels found in these studies suggests that calpain cleavage of Cx50 could reduce the number of functional channel subunits, and lead to the observed decrease in junctional coupling provided by Cx50 during lens fiber maturation. In our studies, we found that the endogenous Cx50 truncations found in the human lens had different effects on GJ conductance. Although C-terminal truncation at the end of TM4 caused no changes in functional properties, truncation at V284 caused channels to be nonfunctional. The impact of the C-terminal cleavage of Cx50 on GJ coupling in the human lens is thus likely dependent on the relative abundances of the two Cx50 cleavage sites.

There are no studies on the effects of endogenous Cx46 truncations in the lens. Our results indicate that C-terminal cleavage of Cx46 does not cause a reduction in macroscopic conductance. In addition, both the unitary conductance and ionic permeability of channels formed by truncated Cx46 was similar to the full-length isoform. These results indicate that properties of intercellular communication provided by full-length Cx46 are maintained after fiber cell maturation.

The insensitivity of fiber cell GJs to cytoplasmic acidification has been attributed to C-terminal cleavage of Cx46 and Cx50.[51–53] Although initial studies indicated that cleavage of the C-terminus abolishes pH gating,[41,43] other studies have found that truncated lens connexins remained sensitive to acidification,[45] consistent with our studies. The discrepancy between the different studies could be due to different methodologies used to lower the intracellular pH. However, the fact that 100% CO_2 markedly reduces GJ coupling in transfected mammalian cells expressing truncated channels but not in the lens core[51–53] suggests that pH gating in the lens might involve other PTMs, in addition to C-terminal cleavage. Both Cx46 and Cx50 undergo other PTMs, including phosphorylation and acetylation.[38–40] Identification of other PTMs might help clarify the mechanism underlying the absence of pH gating in the lens. Alternately, the unique microenvironment in the lens, for example, the association of connexins with specialized structures, might affect channel gating differently in the lens.

A limitation of our studies in expression systems is that they do not reproduce the changes that occur to connexin subunits in the lens. In the lens, cleavage of connexin subunits occurs to

preformed channels already present in the membrane, whereas in our studies, expression of cleaved subunits is required to oligomerize and traffic to the membrane. The consequences of age-related increases in the cytoplasmic and N-terminal truncations to GJ coupling in the lens remain to be determined. Previous studies indicate that GJ conductance exhibits a large age-dependent reduction.[55] Thus, one possibility is that these age-related modifications to Cx46 and Cx50, which remove more than 65% of connexin protein, might underlie this decrease in coupling levels in the lens. However, additional studies are necessary to test this hypothesis.

The age-dependent decrease in coupling conductance in the lens causes changes in transport of ions and important metabolites in the lens. Increases in intracellular calcium in fiber cells of the core occur with age.[55] With advancing age, there is also a decrease in the levels of reduced glutathione (GSH) and an increase in oxidized glutathione (GSSG) in the lens core.[20,24,56] The resulting change in the glutathione redox state in the core has been identified as a key factor in the initiation of age-related nuclear cataract. The decrease in GSH has been attributed to the development of a barrier to the diffusion of the antioxidant from the outer cortex to the fiber cells in the lens core.[20] Because GJ channels are permeable to GSH,[19] it is possible that the impediment to diffusion is due to an age-dependent decrease in GJ coupling in mature fiber cells in the aging human lens caused by accumulation of Cx46 subunits truncated at cytoplasmic loop and N-terminal domains. Spatially correlating the age-dependent accumulation of these truncations with decreases in coupling in cells interior to the barrier region with the glutathione redox state and calcium accumulation is a goal of our future studies.

The mechanisms responsible for truncations in Cx46 and Cx50 remain to be determined. Backbone cleavage of Cx50 by the enzymatic action of calpain and other proteases is known to occur in ovine and chick lens.[34–37] Although calpain activity is much lower in the human lens, similar processes might underlie C-terminal truncations in the human lens because of the high enzymatic activity in the outer cortex. However, cleavage in the cytoplasmic loop, which is primarily seen in inner fiber cells, is less likely to be a result of proteases or other enzymes. Cleavage in the cytoplasmic loop occurred at N130 and G119 in Cx46 and Cx50, respectively. Truncation at asparagine residue in Cx46 might occur nonenzymatically via the spontaneous formation of a cyclic succinimide intermediate, as described previously for crystallins[57] and AQP0.[28] The mechanism of truncation at G119 is less clear, but may be due to spontaneous cleavage of the Gly-Thr bond, a process recently described for lens crystallins.[58]

Acknowledgments

Supported by NEI grants EY013462 (KLS) and EY013869 (MS).

Disclosure: **N. Slavi**, None; **Z. Wang**, None; **L. Harvey**, None; **K.L. Schey**, None; **M. Srinivas**, None

References

1. Willecke K, Eiberger J, Degen J, et al. Structural and functional diversity of connexin genes in the mouse and human genome. *Biol Chem*. 2002;383:725–737.
2. Beyer EC, Kistler J, Paul DL, Goodenough DA. Antisera directed against connexin43 peptides react with a 43-kD protein localized to gap junctions in myocardium and other tissues. *J Cell Biol*. 1989;108:595–605.
3. Musil LS, Beyer EC, Goodenough DA. Expression of the gap junction protein connexin43 in embryonic chick lens: molecular cloning ultrastructural localization, and post-translational phosphorylation. *J Membr Biol*. 1990;116:163–175.
4. Paul DL, Ebihara L, Takemoto LJ, Swenson KI, Goodenough DA. Connexin46, a novel lens gap junction protein, induces voltage-gated currents in nonjunctional plasma membrane of *Xenopus* oocytes. *J Cell Biol*. 1991;115:1077–1089.
5. Dahm R, van Marle J, Prescott AR, Quinlan RA. Gap junctions containing alpha8-connexin (MP70) in the adult mammalian lens epithelium suggests a re-evaluation of its role in the lens. *Exp Eye Res*. 1999;69:45–56.
6. Rong P, Wang X, Niesman I, et al. Disruption of Gja8 (alpha8 connexin) in mice leads to microphthalmia associated with retardation of lens growth and lens fiber maturation. *Development*. 2002;129:167–174.
7. White TW, Bruzzone R, Goodenough DA, Paul DL. Mouse Cx50 a functional member of the connexin family of gap junction proteins, is the lens fiber protein MP70. *Mol Biol Cell*. 1992;3:711–720.
8. White TW, Gao Y, Li L, Sellitto C, Srinivas M. Optimal lens epithelial cell proliferation is dependent on the connexin isoform providing gap junctional coupling. *Invest Ophthalmol Vis Sci*. 2007;48:5630–5637.
9. Mathias RT, White TW, Gong X. Lens gap junctions in growth differentiation, and homeostasis. *Physiol Rev*. 2010;90:179–206.
10. Beyer EC, Ebihara L, Berthoud VM. Connexin mutants and cataracts. *Front Pharmacol*. 2013;4:43.
11. Gong X, Li E, Klier G, et al. Disruption of alpha3 connexin gene leads to proteolysis and cataractogenesis in mice. *Cell*. 1997;91:833–843.
12. White TW, Goodenough DA, Paul DL. Targeted ablation of connexin50 in mice results in microphthalmia and zonular pulverulent cataracts. *J Cell Biol*. 1998;143:815–825.
13. Donaldson PJ, Musil LS, Mathias RT. Point: A critical appraisal of the lens circulation model—an experimental paradigm for understanding the maintenance of lens transparency? *Invest Ophthalmol Vis Sci*. 2010;51:2303–2306.
14. Mathias RT, Kistler J, Donaldson P. The lens circulation. *J Membr Biol*. 2007;216:1–16.
15. Gong X, Baldo GJ, Kumar NM, Gilula NB, Mathias RT. Gap junctional coupling in lenses lacking alpha3 connexin. *Proc Natl Acad Sci U S A*. 1998;95:15303–15308.
16. Baruch A, Greenbaum D, Levy ET, et al. Defining a link between gap junction communication, proteolysis, and cataract formation. *J Biol Chem*. 2001;276:28999–29006.
17. Tang Y, Liu X, Zoltoski RK, et al. Age-related cataracts in alpha3Cx46-knockout mice are dependent on a calpain 3 isoform. *Invest Ophthalmol Vis Sci*. 2007;48:2685–2694.
18. Gao J, Sun X, Martinez-Wittinghan FJ, Gong X, White TW, Mathias RT. Connections between connexins, calcium, and cataracts in the lens. *J Gen Physiol*. 2004;124:289–300.
19. Slavi N, Rubinos C, Li L, et al. Connexin 46 (cx46) gap junctions provide a pathway for the delivery of glutathione to the lens nucleus. *J Biol Chem*. 2014;289:32694–32702.
20. Sweeney MH, Truscott RJ. An impediment to glutathione diffusion in older normal human lenses: a possible precondition for nuclear cataract. *Exp Eye Res*. 1998;67:587–595.
21. Kannan R, Yi JR, Zlokovic BV, Kaplowitz N. Molecular characterization of a reduced glutathione transporter in the lens. *Invest Ophthalmol Vis Sci*. 1995;36:1785–1792.
22. Li B, Li L, Donaldson PJ, Lim JC. Dynamic regulation of GSH synthesis and uptake pathways in the rat lens epithelium. *Exp Eye Res*. 2010;90:300–307.
23. Fan X, Liu X, Hao S, Wang B, Robinson ML, Monnier VM. The LEGSKO mouse: a mouse model of age-related nuclear cataract based on genetic suppression of lens glutathione synthesis. *PLoS One*. 2012;7:e50832.

24. Giblin FJ. Glutathione: a vital lens antioxidant. *J Ocul Pharmacol Ther*. 2000;16:121–135.
25. Piatigorsky J. Lens differentiation in vertebrates. A review of cellular and molecular features. *Differentiation*. 1981;19:134–153.
26. Bassnett S. Lens organelle degradation. *Exp Eye Res*. 2002;74:1–6.
27. Lynnerup N, Kjeldsen H, Heegaard S, Jacobsen C, Heinemeier J. Radiocarbon dating of the human eye lens crystallines reveal proteins without carbon turnover throughout life. *PLoS One*. 2008;3:e1529.
28. Ball LE, Garland DL, Crouch RK, Schey KL. Post-translational modifications of aquaporin 0 (AQP0) in the normal human lens: spatial and temporal occurrence. *Biochemistry*. 2004;43:9856–9865.
29. Sharma KK, Santhoshkumar P. Lens aging: effects of crystallins. *Biochim Biophys Acta*. 2009;1790:1095–1108.
30. Wang Z, Obidike JE, Schey KL. Posttranslational modifications of the bovine lens beaded filament proteins filensin and CP49. *Invest Ophthalmol Vis Sci*. 2010;51:1565–1574.
31. Truscott RJ, Friedrich MG. The etiology of human age-related cataract. Proteins don't last forever. *Biochim Biophys Acta*. 2016;1860:192–198.
32. Lampi KJ, Wilmarth PA, Murray MR, David LL. Lens beta-crystallins: the role of deamidation and related modifications in aging and cataract. *Prog Biophys Mol Biol*. 2014;115:21–31.
33. Kistler J, Bullivant S. Protein processing in lens intercellular junctions: cleavage of MP70 to MP38. *Invest Ophthalmol Vis Sci*. 1987;28:1687–1692.
34. Kistler J, Christie D, Bullivant S. Homologies between gap junction proteins in lens heart and liver. *Nature*. 1988;331:721–723.
35. Lin JS, Fitzgerald S, Dong Y, Knight C, Donaldson P, Kistler J. Processing of the gap junction protein connexin50 in the ocular lens is accomplished by calpain. *Eur J Cell Biol*. 1997;73:141–149.
36. Yin X, Gu S, Jiang JX. Regulation of lens connexin 45.6 by apoptotic protease caspase-3. *Cell Commun Adhes*. 2001;8:373–376.
37. Jacobs MD, Soeller C, Sisley AM, Cannell MB, Donaldson PJ. Gap junction processing and redistribution revealed by quantitative optical measurements of connexin46 epitopes in the lens. *Invest Ophthalmol Vis Sci*. 2004;45:191–199.
38. Shearer D, Ens W, Standing K, Valdimarsson G. Posttranslational modifications in lens fiber connexins identified by off-line-HPLC MALDI-quadrupole time-of-flight mass spectrometry. *Invest Ophthalmol Vis Sci*. 2008;49:1553–1562.
39. Wang Z, Han J, Schey KL. Spatial differences in an integral membrane proteome detected in laser capture microdissected samples. *J Proteome Res*. 2008;7:2696–2702.
40. Wang Z, Schey KL. Phosphorylation and truncation sites of bovine lens connexin 46 and connexin 50. *Exp Eye Res*. 2009;89:898–904.
41. Lin JS, Eckert R, Kistler J, Donaldson P. Spatial differences in gap junction gating in the lens are a consequence of connexin cleavage. *Eur J Cell Biol*. 1998;76:246–250.
42. Eckert R. pH gating of lens fibre connexins. *Pflugers Arch*. 2002;443:843–851.
43. Xu X, Berthoud VM, Beyer EC, Ebihara L. Functional role of the carboxyl terminal domain of human connexin 50 in gap junctional channels. *J Membr Biol*. 2002;186:101–112.
44. Stergiopoulos K, Alvarado JL, Mastroianni M, Ek-Vitorin JF, Taffet SM, Delmar M. Hetero-domain interactions as a mechanism for the regulation of connexin channels. *Circ Res*. 1999;84:1144–1155.
45. DeRosa AM, Mui R, Srinivas M, White TW. Functional characterization of a naturally occurring Cx50 truncation. *Invest Ophthalmol Vis Sci*. 2006;47:4474–4481.
46. Wang K, Gu S, Yin X, Weintraub ST, Hua Z, Jiang JX. Developmental truncations of connexin 50 by caspases adaptively regulate gap junctions/hemichannels and protect lens cells against ultraviolet radiation. *J Biol Chem*. 2012;287:15786–15797.
47. Taylor VL, al-Ghoul KJ, Lane CW, Davis VA, Kuszak JR, Costello MJ. Morphology of the normal human lens. *Invest Ophthalmol Vis Sci*. 1996;37:1396–1410.
48. Chai Z, Goodenough DA, Paul DL. Cx50 requires an intact PDZ-binding motif and ZO-1 for the formation of functional intercellular channels. *Mol Biol Cell*. 2011;22:4503–4512.
49. Kronengold J, Trexler EB, Bukauskas FF, Bargiello TA, Verselis VK. Single-channel SCAM identifies pore-lining residues in the first extracellular loop and first transmembrane domains of Cx46 hemichannels. *J Gen Physiol*. 2003;122:389–405.
50. Verselis VK, Trelles MP, Rubinos C, Bargiello TA, Srinivas M. Loop gating of connexin hemichannels involves movement of pore-lining residues in the first extracellular loop domain. *J Biol Chem*. 2009;284:4484–4493.
51. Baldo GJ, Gong X, Martinez-Wittinghan FJ, Kumar NM, Gilula NB, Mathias RT. Gap junctional coupling in lenses from alpha(8) connexin knockout mice. *J Gen Physiol*. 2001;118:447–456.
52. Martinez-Wittinghan FJ, Sellitto C, White TW, Mathias RT, Paul D, Goodenough DA. Lens gap junctional coupling is modulated by connexin identity and the locus of gene expression. *Invest Ophthalmol Vis Sci*. 2004;45:3629–3637.
53. Martinez-Wittinghan FJ, Srinivas M, Sellitto C, White TW, Mathias RT. Mefloquine effects on the lens suggest cooperative gating of gap junction channels. *J Membr Biol*. 2006;211:163–171.
54. Martinez-Wittinghan FJ, Sellitto C, Li L, et al. Dominant cataracts result from incongruous mixing of wild-type lens connexins. *J Cell Biol*. 2003;161:969–978.
55. Gao J, Wang H, Sun X, et al. The effects of age on lens transport. *Invest Ophthalmol Vis Sci*. 2013;54:7174–7187.
56. Lou MF. Redox regulation in the lens. *Prog Retin Eye Res*. 2003;22:657–682.
57. Voorter CE, de Haard-Hoekman WA, van den Oetelaar PJ, Bloemendal H, de Jong WW. Spontaneous peptide bond cleavage in aging alpha-crystallin through a succinimide intermediate. *J Biol Chem*. 1988;263:19020–19023.
58. Lyons B, Kwan AH, Truscott RJ. Spontaneous cleavage of proteins at serine and threonine is facilitated by zinc. *Aging Cell*. 2016;15:237–244.

Investigative Ophthalmology & Visual Science